Aalborg Universitet

Advanced Nonlinear Control of A Grid-Connected Photovoltaic Power System Using N-Cascaded H-Bridge Multilevel Inverters

H. Katir*, A. Abouloifa *, I. Lachkar**, K. Noussi*, F. Giri***, J. M. Guerrero****

*TI Lab, Faculty of Sciences Ben M'sick, University Hassan II of Casablanca, BP 7955 Casablanca Morocco.
(Corresponding author: katir.hanane@gmail.com)
**ESE Lab, ENSEM of Casablanca, University Hassan II of Casablanca, BP 7955 Casablanca Morocco.
*** LAC Lab, EA 7478, University of Caen, Basse-Normandie, 14032 Caen, France.
****Department of Energy Technology, AAU, 9220 Aalborg East, Denmark.

Abstract: The present paper discusses the modelling and the nonlinear control of a DC/AC conversion system composed of photovoltaic arrays, boost converters, DC bus capacitors, N-cascaded H-bridge multilevel inverters (CHBMI) and an L-filter linked to a single-phase grid. This work aims at achieving threefold control objectives: i) regulating the voltages across the PV panels in order to extract the available maximum power, ii) guaranteeing a unitary power factor (UPF) by forcing the grid current to be sinusoidal and in phase with the electric network voltage, iii) controlling the DC-link voltages to track their given references. The achievement of these objectives is done thanks to a regulator based on a multi-loop structure. Indeed, on one hand, each panel is individually controlled to track the maximum power point; on the other hand, two cascaded loops aim at ensuring a satisfactory power factor correction and DC-link voltages regulation. The proposed regulator is developed using the nonlinear backstepping approach and some tools from Lyapunov stability. The simulation results, obtained using MATLAB/SIMULINK/ SimPowerSystems environment, prove that the synthesized regulator meets its objectives and presents interesting performance in terms of tracking and regulation.

Keywords: Cascaded H-bridge multilevel inverter, PV system, Nonlinear control, PFC, Lyapunov, Backstepping approach, Grid.

1. INTRODUCTION

The increasing demand on energy is one of the encouraging factors to look for an alternative of classical sources like fossil fuels which represent a harmful source of energy threatening the environment. Therefore, renewable energy, especially solar energy has been introduced as a solution to defeat the short-comes of fossil fuels (Noussi et al., 2019). In fact, photovoltaic systems offer countless advantages, in terms of clean energy generation, being noiseless and environmental-friendly, as well as affording the opportunity to construct and extend any size, based on energy requirements.

Actually, not all PV sources of energy work similarly, though put under the same conditions. One of the hinders facing researchers using PV systems is the PV mismatch caused by the unequal delivered irradiance, dissimilar temperature and the age of the PV panels (Xiao et al., 2013). Thus, the maximum power points (MPPs) may not be identical to each PV module. Regarding this issue, this paper suggests the control of each PV module independently in order to track its own maximum power point.

This paper exploits the benefits of solar energy by using PV modules and the advantages of the cascaded topology present in the CHBMI. The studied system taking part in this work is composed of N sub-systems that contain N-PV arrays

delivering input voltages to N converters of DC/DC boost type which are linked to DC-link voltages. In view of the fact that each H-bridge inverter requires to be connected to an isolated DC source, it is necessary to link each sub-system to an H-bridge inverter. All H-bridge inverters are associated in cascade and inject a low THD sinusoidal current in the grid via an L-filter.

Some research papers have eliminated the DC-DC stage in an attempt to lessen the size of the system. However, this elimination entails increasing the dimensions of the PV panels, and using suitable transistors which could support operating in medium to high voltages. Whereas, using a boost converter offers the opportunity to minimize the number of the PV modules (Wang et al., 2016). In literature, many researchers limited their studies on using an H-bridge inverter, avoiding the cascade topology and its returns in terms of being able to work with high power demanding applications and injecting a low THD current using a low dimensional filter.

Taking into consideration the importance of the CHBMI, many control techniques have been suggested, namely the proportional–integral (PI) controller in (Paul Raj and Meenakshi Sundaram, 2016), the sliding mode controller in (Gupta et al., 2010), the PI and Fuzzy logic controller (FLC) in (Kannan et al., 2017), the nonlinear and adaptive backstepping controllers in (Katir et al., 2019), etc.

In this paper, the system under investigation is composed of N different sub-systems. All of them work together towards the realization of three main objectives:

i. extracting the maximum power provided by the PV modules.

ii. controlling the grid current and ensuring a unitary power factor (UPF) in the grid side.

iii. regulating the DC-link voltage to track a fixed reference.

The achievement of the above objectives, in regard to the nonlinear electrical characteristics of the system, requires the design of a multi-loop regulator using the nonlinear backstepping approach and some tools from Lyapunov stability. On the DC side, the developed control strategies deal with providing the maximum available power by regulating the voltage across the N-PV panels, and adjusting the DC-link voltages to track a given reference. Whereas on the AC side, the used nonlinear controller forces the grid current to be in phase with the grid voltage, ensuring this way a unitary power factor (UPF). The studied system can take part in many industrial applications and bring tremendous outcomes, in terms of precision, robustness and efficiency.

This paper is organized as follows: the description and mathematical modelling of the PV systems, boost converters and the cascaded H-bridge multilevel inverter are discussed in Section II. Section III proposes the controller design. Section IV introduces the simulation results of the studied system verifying the above objectives and Section V provides the conclusions. Finally, a list of consulted references is given below the conclusion.
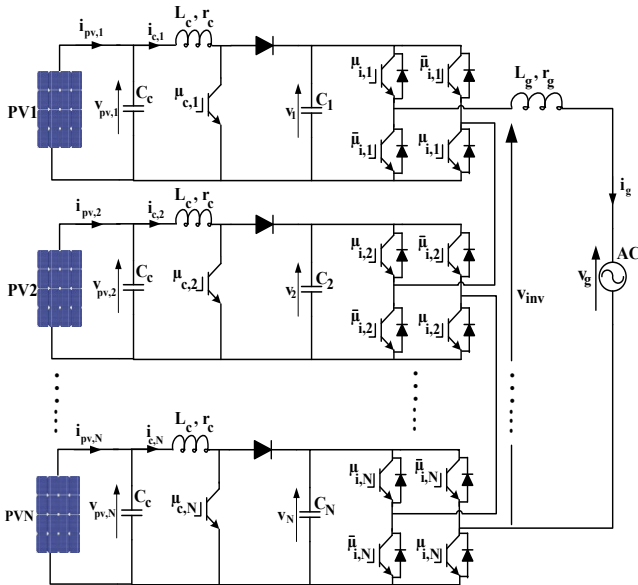

Fig. 1. Circuit schematic of the overall system

2. SYSTEM DESCRIPTION AND MODELLING

2.1 System Description

The studied system is formed using N sub-systems (Fig.1.). Each one of them contains a PV module, a boost DC-DC converter and a capacitor connected to the DC-side of the H-bridge inverters. These latter are linked in cascade so as to

generate a multilevel output voltage able to inject a low THD current to the grid via an L-filter.

2.2 System Modelling

Applying the standard Kirchhoff's laws to the circuit shown in figure 1, the instantaneous mathematical model describing the system can be expressed by the following nonlinear differential equations:

$$C_c \frac{dv_{pv,k}}{dt} = i_{pv,k} - i_{c,k} \tag{1a}$$

$$L_c \frac{di_{c,k}}{dt} = -r_{c,k}i_{c,k} + v_{pv,k} - (1-\mu_{c,k})v_k \tag{1b}$$

$$C_k \frac{dv_k}{dt} = (1-\mu_{c,k})i_{c,k} - 2\mu_{i,k}i_g \tag{1c}$$

$$L_g \frac{di_g}{dt} = -r_g i_g - v_g + \sum_{k=1}^{N} 2\mu_{i,k}v_k \tag{1d}$$

where $k = 1,2,...,N$; $v_{pv,k}$ and $i_{pv,k}$ are the voltage and the current of the PV arrays; v_k is the kth DC-link voltage, i_g and v_g designate the current and voltage of the grid, respectively; $i_{c,k}$ represents the input current of the boost converters. $\mu_{c,k} \in \{0,1\}$ and $\mu_{i,k} \in \{-1,1\}$ are the switching functions of the kth DC/DC boost converter and the kth H-bridge inverter, respectively.

Therefore, the number of voltage-levels N_{level} provided by an N-cells cascaded H-bridge converter can be written as:

$$N_{level} = 2N + 1 \tag{2}$$

Since $\mu_{c,k}$ and $\mu_{i,k}$ represent binary control input signals and take part in the switched model of equations (1a–d), the design of continuous control laws can not be done appropriately. To face this challenge and be able to control the system under investigation, the averaged model of the suggested topology can be expressed as follows:

$$C_c \dot{x}_{1,k} = i_{pv,k} - x_{2,k} \tag{3a}$$

$$L_c \dot{x}_{2,k} = -r_{c,k}x_{2,k} + x_{1,k} - (1-u_{c,k})x_{3,k} \tag{3b}$$

$$C_k \dot{x}_{3,k} = (1-u_{c,k})x_{2,k} - 2u_{i,k}x_4 \tag{3c}$$

$$L_g \dot{x}_4 = -r_g x_4 - v_g + \sum_{k=1}^{N} 2u_{i,k}x_{3,k} \tag{3d}$$

where $x_{1,k}$ and $x_{2,k}$ are the voltage across the PV arrays and the input current of the boost converters, respectively; $x_{3,k}$ denotes the DC-link voltages and x_4 is the grid current.

3. CONTROLLER DESIGN

Taking into account the nonlinearity nature of the structure under study and in order to attain the regulation objectives, a controller design of four control units is developed as shown in figure 2.

This section concerns the regulator design, in order to reach three objectives simultaneously. First, we seek at assuring the PV modules to work in the maximum power points MPPs. Second, we desire to control the grid current aiming at

delivering it to the grid with a unitary power factor (UPF) and third, we intend to regulate the voltages across the DC-link to be used as inputs by the CHBMI.

The controller design incorporates a host of loops: N-voltage loops that ensure the performance to take place at the maximum available power points (MPPs); a current loop to adjust the grid current so as to be in phase with the grid voltage as well as to follow a given current reference, and N outer-loops that control the voltages across the DC-link.
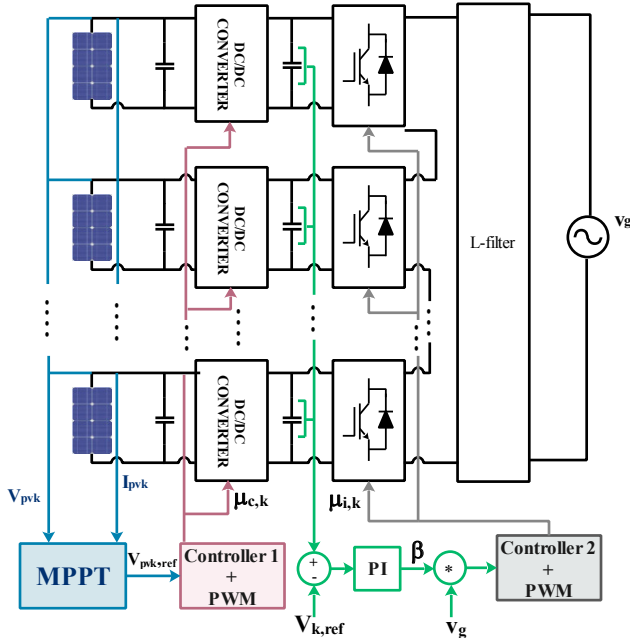

Fig. 2. Schematic diagram of the controller design

3.1 PV voltage regulator design(MPPT objective)

The parameters of the PV modules rely on the variation of the insolation, the temperature and the load. Therefore, applying the MPPT is obligatory to control the operating voltage to be around the maximum power point and to get the desired output voltage with the minimum possible number of solar panels (Bhandari et al., 2014). To achieve the above objectives, the well-known P&O "perturb and observe algorithm" technique is used since it is simpler and needs fewer measured parameters. The PV voltage and the PV current are the input signals of the P&O block leading to a PV reference voltage in the output. This latter is employed as a reference by the boost regulator (Aourir et al., 2020 ; Abouloifa et al., 2018). The aim behind using the PV arrays is to deliver DC voltages to the studied system. The objective of the present control technique is to get a DC voltage across the output of every solar array close to its MPPs, so as to control the parameters of each DC/DC boost converter which takes place to increase the PV level voltage to be used later by the CHBMI. The regulation technique allowing the fulfilment of this objective is the backstepping technique. Since the subsystems under investigation have a relative degree of two, the backstepping approach is done in two steps so as to reach the control laws.

Step1: Stabilization of the sub-systems (3a)

Let us introduce the first tracking error:

$$e_{1,k} = C_c(x_{1,k} - x_{1,k}^*) \tag{4}$$

Using (3a) and (4), time-derivation yields to the following tracking error dynamics:

$$\dot{e}_{1,k} = i_{pv,k} - x_{2,k} - C_c \dot{x}_{1,k}^* \tag{5}$$

Taking into concern that the Lyapunov function should be positive and its derivative must be negative, we make the choice of the following candidate Lyapunov function:

$$V_{1,k} = 0.5\, e_{1,k}^2 \tag{6}$$

Indeed, its time derivative leads to:

$$\dot{V}_{1,k} = e_{1,k}\dot{e}_{1,k} = -c_1 e_{1,k}^2 < 0 \tag{7}$$

where c_1 is a positive design parameter.

Considering that $x_{2,k}$ is the kth virtual control input signal and in respect to the Lyapunov function (6) and its dynamic (7), the kth stabilizing function of the subsystems (3a) is obtained as follows:

$$x_{2,k}^* = c_1 e_{1,k} + i_{pv,k} - C_c \dot{x}_{1,k}^* \tag{8}$$

As $x_{2,k}$ is not the actual control law, we define the second tracking error:

$$e_{2,k} = L_c(x_{2,k} - x_{2,k}^*) \tag{9}$$

Using (8) and (9), equation (5) becomes:

$$\dot{e}_{1,k} = -c_1 e_{1,k} - \frac{e_{2,k}}{L_c} \tag{10}$$

Consequently, time-derivation of the Lyapunov function becomes:

$$\dot{V}_{1,k} = -c_1 e_{1,k}^2 - \frac{e_{1,k} e_{2,k}}{L_c} \tag{11}$$

Step2: Stabilization of the sub-systems (3b)

Reaching the control laws, which aim at regulating the voltages across the PV modules as well as boosting the input voltages, requires the error variables e_1 and e_2 to fade away.
Using equation (3b) and (9), time-derivation of the second tracking error results to be:

$$\dot{e}_{2,k} = -r_{c,k}x_{2,k} + x_{1,k} - (1-u_{c,k})x_{3,k} - L_c\dot{x}_{2,k}^* \tag{12}$$

Let us consider the following choice of the augmented Lyapunov function:

$$V_{2,k} = 0.5 e_{2,k}^2 + V_{1,k} \tag{13}$$

Using equations (11) and (13), one gets:

$$\dot{V}_{2,k} = -c_1 e_{1,k}^2 + e_{2,k}\dot{e}_{2,k} - \frac{e_{1,k} e_{2,k}}{L_c} \tag{14}$$

Our aim is to make $\dot{V}_{2,k}$ negative by the next choice:

$$\dot{e}_{2,k} - \frac{e_{1,k}}{L_c} = -c_2 e_{2,k} < 0 \tag{15}$$

Noting that c_2 is a positive regulator parameter.

The combination of equations (12) and (15) lead to the control laws given by the expression:

$$u_{c,k} = 1 + \frac{1}{x_{3,k}}\left(r_{c,k}x_{2,k} - c_2 e_{2,k} - x_{1,k} + L_c\dot{x}_{2,k}^* + \frac{e_{1,k}}{L_c}\right) \tag{16}$$

As far as it concerns the control of the N boost DC-DC converters, the generation of N suitable gate signals occurs through applying the control laws expressed in (16) to PWM generators.

Proposition 3.1

In regards to the control laws (16) and the averaged mathematical model described by equations (3a) and (3b), the dynamic behaviour of the kth closed loop system, in the $(e_{1,k}, e_{2,k})$ coordinates, can be expressed as:

$$\begin{pmatrix} \dot{e}_{1,k} \\ \dot{e}_{2,k} \end{pmatrix} = \begin{pmatrix} -c_1 & -1/L_c \\ 1/L_c & -c_2 \end{pmatrix} \begin{pmatrix} e_{1,k} \\ e_{2,k} \end{pmatrix} \tag{17}$$

As a result, the error variables $(e_{1,k}, e_{2,k})$ globally asymptotically vanish.

3.2 Grid current regulator (PFC objective)

The reason behind the regulation of the grid current is to force the grid current to track the reference $x_4^* = \beta v_g$, where β is a real positive signal to be defined in the next subsection. This regulator aims at injecting a sinusoidal current to the grid with the minimum harmonics possible and assuring a unitary power factor. To achieve these objectives, the used regulation technique goes through these steps:

Using equation (3d) to examine the performance of the error between the desired reference current and the actual current, the error undergoes:

$$e_g = L_g(x_4 - x_4^*) \tag{18}$$

Deriving the error, it follows from (3d) that:

$$\dot{e}_g = -r_g x_4 - v_g + \sum_{k=1}^{N} 2u_{i,k} x_{3,k} - L_g \dot{x}_4^* \tag{19}$$

In order to realize the negativity of the derivative and ensure that the system is globally asymptotically stable, the following choice is made:

$$\dot{e}_g = -\delta_g e_g \tag{20}$$

where δ_g is a real positive controller parameter.

As the aim of the suggested regulator is to find appropriate control laws able to achieve the desired objectives, the Lyapunov function can be selected as follows:

$$W = 0.5e_g^2 \tag{21}$$

From equations (19), (20) and (21), the control laws turn out to be as follows:

$$\sum_{k=1}^{N} u_{i,k} = \frac{1}{2x_{3,k}} \left[-\delta_g e_g + r_g x_4 + v_g + L_g \dot{x}_4^* \right] \tag{22}$$

If one considers that all CHBMI behave identically, the control law of each inverter results to be:

$$u_{i,k} = \frac{1}{2Nx_{3,k}} \left[-\delta_g e_g + r_g x_4 + v_g + L_g \dot{x}_4^* \right] \tag{23}$$

3.3 DC Link voltage regulator

The DC link voltage regulator seeks at designing control laws which regulate the DC-link voltage across each capacitor feeding an H-bridge inverter, in a way that these capacitors generate DC constant voltages. To reach this objective and taking into account that the derivative of the signal β must be available, a filtered PI regulator is designed. The proposed controller's input is the difference between the reference voltage, chosen by the instructor, and the sum of the N-capacitors' voltages; whereas, the output of the filtered PI regulator represents the factor β.

The control law β is expressed as:

$$\beta = L^{-1}\left[\frac{1}{1+\tau s}\left(K_p + \frac{K_i}{s} \right) \right] \tag{24}$$

where L^{-1} designates the well-known inverse Laplace transform; and τ, K_p and K_i are positive design parameters.

4. SIMULATION

To check the performance and prove evidence of the designed regulator, the studied system is implemented in MATLAB/SIMULINK/ SimPowerSystems environment. The simulation is done with the choice of k=3, in order to limit the analysis on three cascaded H-bridge cells. Each of them is linked, on one side, to a DC bus capacitor, a boost converter and a PV system. The PV arrays used in this study (1Soltech 1STH-220-P) contain four strings connected in parallel. Each string is formed by two modules linked in series. On the AC side, the three cascaded H-bridge inverters are tied in cascade delivering a seven level voltage to an L-filter. The output of the whole structure is a current injected to the grid respecting a satisfactory power factor correction (PFC).

The system and controller's simulation parameters can be found in table I and table II.

Table I
System characteristics

Parameters	Symbols	Values
Network	v_g, f_n	220V/50Hz
Boost	C_c, L_c, r_c	100µF,3mH, 50mΩ
L-filter	L_g, r_g	2mH, 50mΩ
DC-Link Capacitance	$C_1 = C_2 = C_3$	2mF
Cascaded Number	N_c	3
PWM frequency	f_{PWM}	10 kHz

Table II
Controller parameters

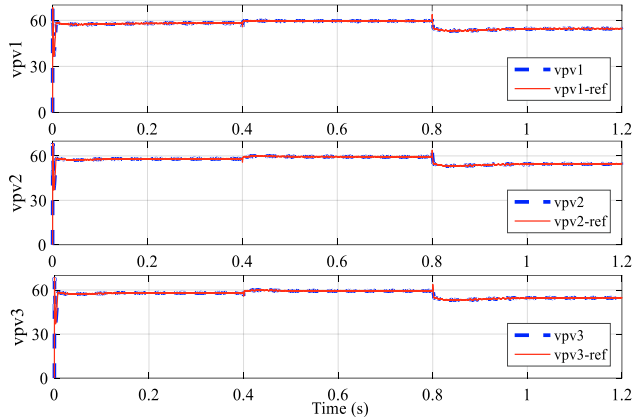| Parameters	Symbols	Values
PV Voltage regulator	c_1, c_2	8000, 15000
DC Link regulator	k_p, k_i, τ	5e-4, 4e-3, 5e-3
PFC regulator	δ_g	2000000

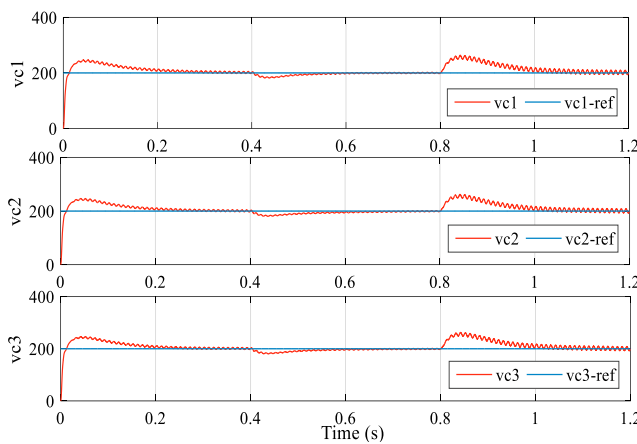Fig. 3. PV voltages and their references

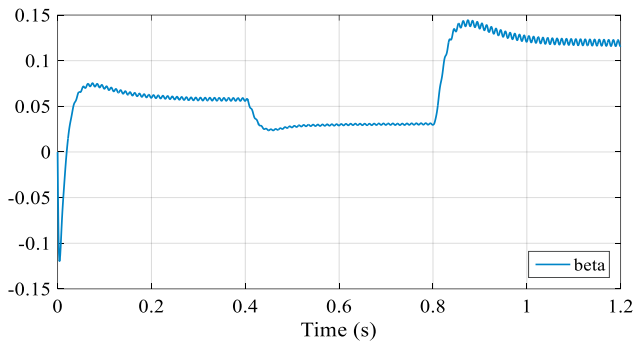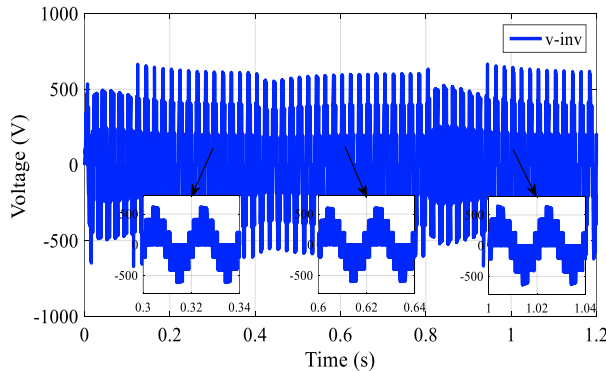Fig. 4. DC-Link voltages and their references

Fig. 5. The control signal β

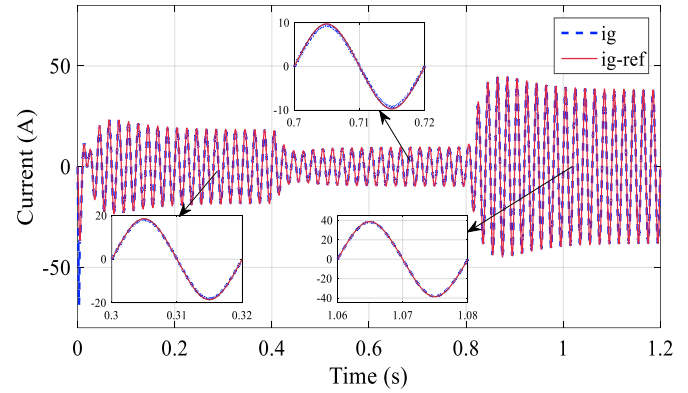Fig. 6. Three cascaded H-bridge inverters' voltage output

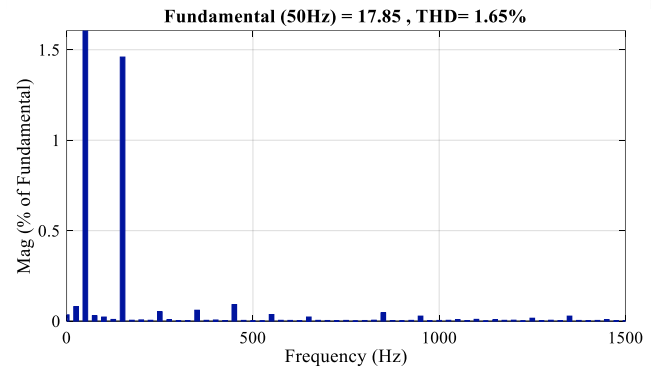Fig. 7. The grid current and its desired reference

Fig. 8. FFT analysis of the grid current
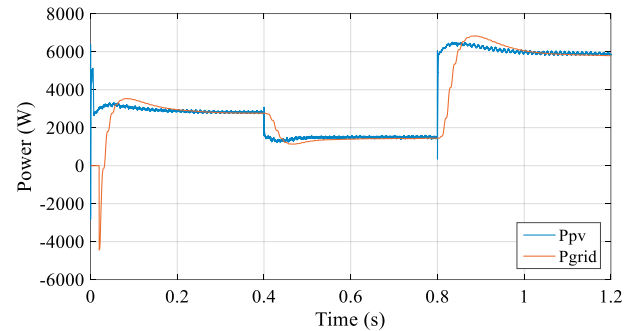

Fig. 9. PV and grid powers
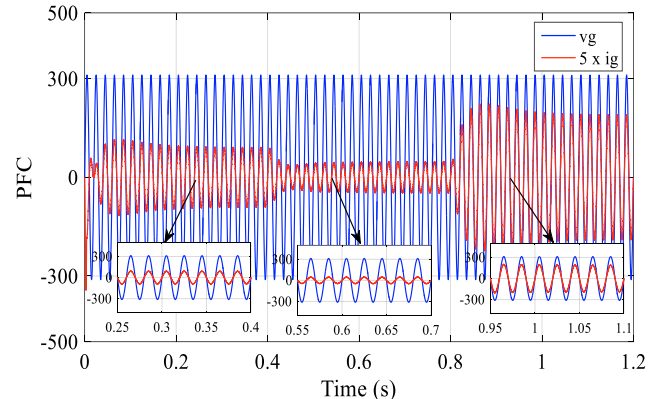

Fig. 10. PFC checking

In the simulation, the PV modules are examined under standard conditions where the sun irradiance equals 1000W/m² and the temperature is specified at 25 °C. It is clearly noticeable that the PV voltages of the three PV arrays reach their MPPs. Moreover, one can observe in figure 3 that the tracking of the PV reference voltages is perfect.

The developed multi-loop nonlinear controller goes through a test of robustness by changing the irradiations of the sun received by the panels. In fact, these variations can also occur as far as it concerns temperature, but it attracts more interest in terms of behavior and tracking performance to change the irradiations of the solar arrays rather than temperature. This variation happens in respect to the standard temperature 25°C as follows:

Table III

Irradiation variations

Time span (s)	[0 0.4]	[0.4 0.8]	[0.8 1.2]
Irradiation (KW/m^2)	1	0.8	1.5

Even with the irradiations change, figure 3 proves that the PV voltages track their references efficiently. The control of the DC-link forces the voltage across each capacitor to follow its reference fixed at 200V as shown in figure 4 despite the irradiations' change. Figure 5 represents the variation of the tuning ratio signal β.

One of the objectives of the inner loop of the subsystem (3d) is to obtain a sinusoidal current that tracks its reference coming from the outer loop. The tracking performance of this subsystem is witnessed in figure 7, where the current reaches its given reference rapidly in spite of the changes of the irradiations. It is worth noting that the grid current's amplitude correlates with the irradiations' level.

Since the simulation tests the performance of the system with three H-bridge inverters, it is predicted to have a seven level voltage signal. Figure 6 confirms the predictions and validates the results of the regulator.

 An FFT analysis is also done to check the THD of the grid current. Figure 8 proves that the THD of the grid current complies with the standard norms (the Australian standard (AS_4777-2005) and IEEE 929-2000 standard (IEEE_929-2000)) (Du et al., 2013), which state that a current's THD is restricted to less than 5%.

Figure 9 illustrates that the generated PV power goes hand in hand with the absorbed grid power, leading the system to be equilibrated and stable.

The main objective of this study is to be able to inject a sinusoidal current with respect to a unitary power factor, where the grid current is in phase with the grid voltage. Figure 10 demonstrates the achievement of this objective.

5. CONCLUSIONS

This paper addresses the problem of the regulation of a complete DC/AC conversion system. The detailed control strategies' performance is analyzed and verified in the simulation section. The simulation results prove the efficiency and robustness of this conversion chain as it can deliver quality sinusoidal current to the grid with a minimized number of input PV arrays and a satisfactory power factor correction. It is worth noting that the used regulator in the N

subsystems offers fruitful results and leads to the fulfilment of the control objectives.

REFERENCES

Abouloifa, A., Aouadi, C., Lachkar, I., Boussairi, Y., Aourir, M., Hamdoun, A., (2018). Output-Feedback Nonlinear Adaptive Control Strategy of the Single-Phase Grid-Connected Photovoltaic System. Journal of Solar Energy, 1–14.

Aourir, M., Abouloifa, A., Lachkar, I., Aouadi, C., Giri, F., Guerrero, J.M., (2020). Nonlinear control and stability analysis of single stage grid-connected photovoltaic systems. International Journal of Electrical Power & Energy Systems 115, 105439.

Bhandari, B., Poudel, S.R., Lee, K.-T., Ahn, S.-H., (2014). Mathematical modeling of hybrid renewable energy system: A review on small hydro-solar-wind power generation. Int. J. of Precis. Eng. and Manuf.-Green Tech. 1, 157–173.

Du, Y., Lu, D.D.-C., James, G., Cornforth, D.J., (2013). Modeling and analysis of current harmonic distortion from grid connected PV inverters under different operating conditions. Solar Energy 94, 182–194.

Gupta, R., Ghosh, A., Joshi, A., (2010). Multiband Hysteresis Modulation and Switching Characterization for Sliding-Mode-Controlled Cascaded Multilevel Inverter. IEEE Trans. Ind. Electron. 57, 2344–2353.

Kannan, C., Mohanty, N.K., Selvarasu, R., (2017). A new topology for cascaded H-bridge multilevel inverter with PI and Fuzzy control. Energy Procedia 117, 917–926.

Katir, H., Abouloifa, A., Noussi, K., Lachkar, I., (2019). Adaptive Backstepping Control Of Cascaded H-Bridge Multilevel DC/AC Converters, in: 2019 4th World Conference on Complex Systems (WCCS). IEEE, pp. 1–6.

Noussi, K., Abouloifa, A., Katir, H., Lachkar, I., (2019). Modeling and Control of a Wind Turbine Based On a Doubly Fed Induction Generator, in: 2019 4th World Conference on Complex Systems (WCCS). IEEE, pp. 1–5.

Paul Raj, M.M., Meenakshi Sundaram, S.S., (2016). Cascaded H-Bridge Five-Level Inverter for Grid-Connected Photovoltaic System Using Proportional–Integral Controller. Measurement and Control 49, 33–41.

Wang, L., Zhang, D., Wang, Y., Wu, B., Athab, H.S., (2016). Power and Voltage Balance Control of a Novel Three-Phase Solid-State Transformer Using Multilevel Cascaded H-Bridge Inverters for Microgrid Applications. IEEE Trans. Power Electron. 31, 3289–3301.

Xiao, B., Hang, L., Riley, C., Tolbert, L.M., Ozpineci, B., (2013). Three-phase modular cascaded H-bridge multilevel inverter with individual MPPT for grid-connected photovoltaic systems, in: 2013 Twenty-Eighth Annual IEEE Applied Power Electronics Conference and Exposition (APEC). IEEE, pp. 468–474.